Investigating the Outflows and Shocks of HOPS 361

Time Request:

SOFIA: GREAT 6.5 hours
HST: WFC3 in five filters (F126N, F128N, F130N, F164N, and F167N) in 12 orbits

Science Team: Nicole Karnath (SOFIA/USRA), Tom Megeath (UToledo), Dan Watson (URochester), Nolan Habel (UToledo), Amelia Stutz (UdeC), John Tobin (NRAO), Manoj Puravankara (TIFR), Mayank Narang (TIFR), Archana Soam (SOFIA/USRA), David Neufeld (JHU), Neill Reid (STScI), Riwaj Pokhrel (UToledo), Steve Goldman (STScI), Will Fischer (STScI), Yu Cheng (UVA), Ian Stephens (CfA), Simon Coude (SOFIA/USRA), Randolf Klein (SOFIA/USRA), Joel Green (STScI), Megan Reiter (UK ATC), Curtis DeWitt (SOFIA/USRA), Ed Montiel (SOFIA/USRA), Adele Plunkett (NRAO), Ed Chambers (SOFIA/USRA)

Abstract: We propose a HST near-IR + SOFIA far-IR study of NGC 2071, a system of at least two outflows from a small group of intermediate to low luminosity stars. Protostellar outflows are ubiquitous part of the star formation process. They provide a record of variable accretion onto stars, have significant impact on the surrounding molecular cloud, and may disrupt or trigger star formation in molecular clouds. Intermediate-luminosity ($30 \leq L_{bol} \leq 1000 L_{\odot}$) protostars bridge the gap between low- and high-mass star formation, forming stars with masses between 2 and 10 $M_{\odot}$ stars (Di Francesco et al. 1997; Mannings & Sargent 2000). Outflows from these systems of protostars have a significant impact on the surrounding ISM, may play an important role in cloud evolution, and are an important laboratory for understanding the origin of far-IR line emission from outflows. Shock-excited emission lines in the near- and far-IR can be used to study the energetics of outflows and their impact on the surrounding cloud. In this study, WFC3/IR images of [FeII] and Paschen β lines will trace J-type shocks in the near-IR. A comparison of these data to WFC3/IR imaging in the F160W band from 2009 will be used to derive proper motions. The intensity of these lines will provide estimates of the mechanical luminosity of the line. SOFIA 4GREAT will trace emission from far-IR transitions of [OI] and four additional CO transitions tracing shock heated gas. These lines will provide both radial velocities of the shocked emission as well as measurements of the mass flow and heating by shocks and UV radiation. The combined data will provide 3D space motions of the knots of shock accelerated gas where the outflow is interacting with the surrounding molecular cloud. Additionally, shock velocities and mass and energy momentum flows through the shocks will provide one of the most detailed measurements of the feedback from a system of protostars to date. The observations of this relatively nearby system (420 pc, Kounkel et al. 2017) will provide unique information on the outflows in a region that is being increasingly well studied through SOFIA FORCAST and HAWC+ observations, making it a well-characterized template for intermediate-mass star formation.

Introduction: While jets and outflows from protostars have been extensively studied, new approaches to study these objects in the near-IR, far-IR, and sub-millimeter with HST, SOFIA, and ALMA, respectively, can provide a new and detailed picture of the kinematics and energetics of outflows, particularly in crowded systems launching multiple outflows. Accretion driven molecular outflows/jets are essential components of the star formation process across the mass spectrum providing a history of accretion, carrying off the angular momentum of the accretion gas, and are the main sources of mechanical feedback onto the parental cloud (Nakamura & Li 2007), which play a major role in determining the IMF and contributing to the low star formation efficiency of molecular clouds. Simulations of star formation cannot resolve all the relevant spatial and temporal scales needed to simulate the generation of feedback in disks and the effect of the feedback on the surrounding clouds (e.g., Machida 2017). Observational touchstones are are needed to quantify the flows of mass and momentum launched by protostars and the details of their interaction with the surrounding cloud.

Intermediate-mass protostars are essential targets of star formation because they provide the link between low- and high-mass stars (Di Francesco et al. 1997; Mannings & Sargent 2000). Jets and outflows span several orders of magnitude in momentum flux, mechanical luminosity, and their impact on their natal molecular cloud (Figure 1). High-mass protostellar outflow properties scale up from low-mass protostellar outflows, and outflow momenta range from 10^{-2} to several $M_\odot$ km/s, outflow energies range between 10^{42} and 10^{45} erg, and outflow mechanical forces range from 10^{-7} to 10^{-2} $M_\odot$ yr $^{-1}$ km/s. The few outflow forces measured for intermediate-mass protostars fall between high- and low-mass protostellar outflows. For example, van Kempen et al. (2016) found that six intermediate-mass protostars had outflow forces 10 to 300 times higher than low-mass protostars in Bontemps et al. (1996) and were consistent with the low-end values of high-mass sources (10^{-4} $M_\odot$ yr^{-1} km/s).

The outflow feedback also clears the natal envelope halting the infall process (Offner & Arce 2014) and drives turbulence at small and large scales. Feedback from outflows reduces the overall star-formation efficiency, particularly on the smaller spatial scales (Figure 1, see Frank et al. 2014). However, observational constraints on the large-scale energy and momentum injected into molecular clouds from feedback is limited. Numerical simulations have been carried out but with differing initial conditions, assumptions, and resolutions that affect the outcome (e.g., Kuiper et al. 2015).

Far-IR emission lines have emerged as an important tracer of outflows. These lines are diagnostics of warm and hot molecular and atomic gas (Watson et al. 1980; Storey et al. 1981; Giannini et al. 2001; Nisini et al. 2002) that can characterize the density, temperature, molecular abundances, and spatial extent of the emitting region (Watson et al. 1985; Draine et al. 1983; Hollenbach & McKee 1989; Kaufman & Neufeld 1996). *Herschel*/PACS spectra detected lines of [OI], CO, and H_2O in protostellar outflows, including the NGC 2071 outflow (Manoj et a. 2013, 2016; Karska et al. 2013, 2018; Gonzales-Garcia et al. 2016; Matuszak et al. 2015). The high-J CO lines ($14 \leq J_{up} \leq 45$) are particularly prominent in the spectra of protostars. Manoj et al. (2016) found a strong correlation between the total luminosity in these CO lines, L_{CO}^{FIR}, and the L_{bol} of the protostar. No other significant correlation was found between L_{CO}^{FIR} and evolutionary indicators. Manoj et al. (2013) argued that most of the luminosity in the far-IR CO

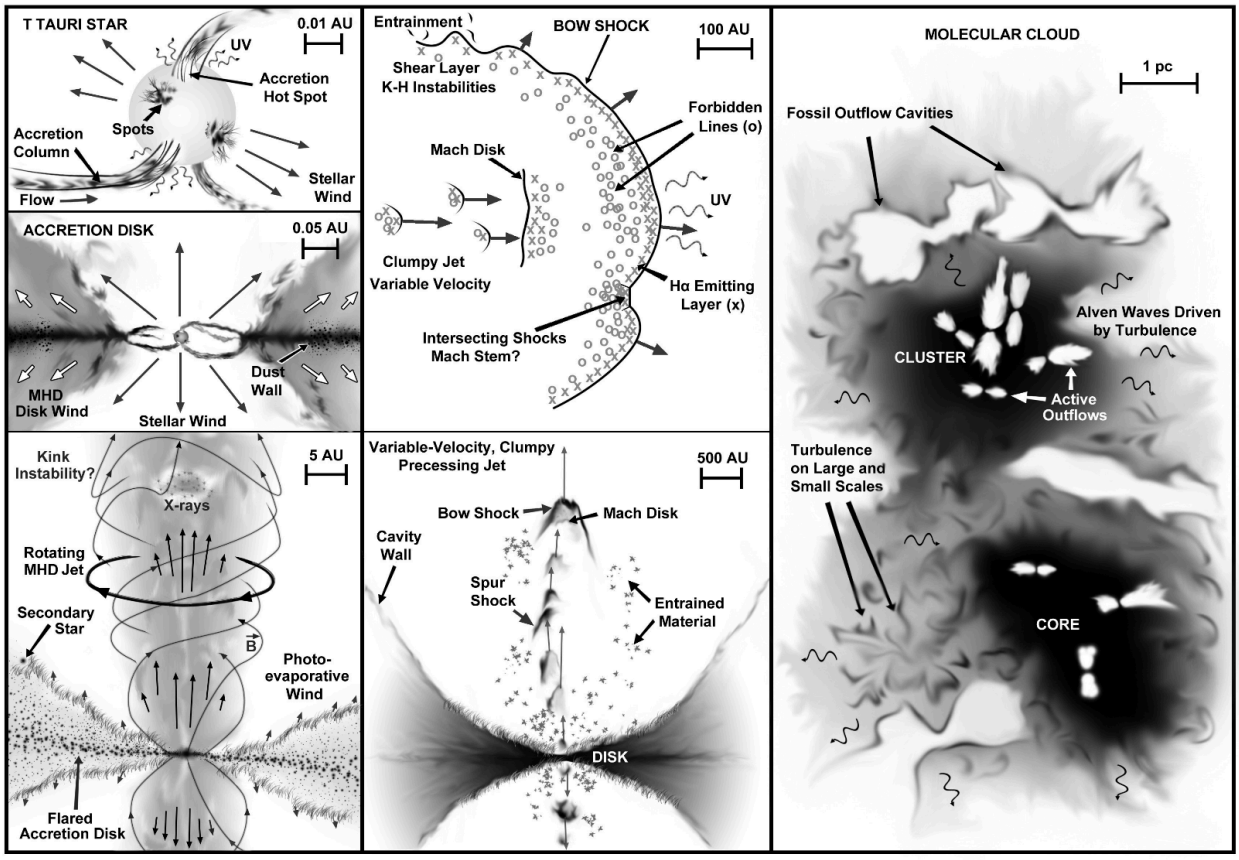

Figure 1: *A schematic view of jets and outflows from Frank et al. (2014). The panels step through the orders of magnitude in scale of jets and outflows and their feedback on the surrounding cloud.*

lines come from shock-heated hot (100-2000 K) gas in the outflow. They argue that these lines track the mechanical luminosity of the outflows; other studies of protostars have also shown that L_{CO}^{FIR} is ~30-40% of the total far-IR cooling (Karska et al. 2013; Lee et al. 2014).

Low-J CO lines ($J_{up} \leq 3$) mapped with ground-based (sub)-millimeter telescopes such as ALMA primarily trace the gas from the surrounding molecular cloud that was swept up or entrained in the outflow. These give a time-averaged picture outflow over the lifetime of the protostar. In contrast, the far-IR lines give a relatively instantaneous measurement of the mechanical luminosity of the outflow. Furthermore, [OI] measurements can measure the mass flow across J-type shocks and, when combined with velocity information, give an instantaneous measure of the momentum flow. The multiple CO transitions that will be observed with 4GREAT and the existing H_2 emission from *Spitzer* lie in the turbulent boundary layer just outside the outflow cavity wall, and in the "cloud shock" past the wind shock, representing the supersonic acceleration of ambient material. Together, these far-IR lines promise a relatively direct measurement of the current impact of the outflow on the cloud.

Goals: The goal of this project is to measure 3D space motions of knots and quantify the mechanical feedback from accretion driven outflows in a well studied region of Orion. Figure 2 shows the 2009 WFC3/IR F160W image of NGC 2071 with the individual protostars and outflow components identified in the region. This region, just north of the NGC 2071 reflection nebulae, contains a cluster of seven young stellar objects in a 2000 AU diameter region with a total luminosity of 500 $L_\odot$ as shown in X-ray, radio, and IR data (see Figure 3, e.g.,

Skinner et al. 2009; Furlan et al. 2016; Tobin et al. 2020). FORCAST imaging at 19.7 and 25.3 micron shows the luminosity is dominated by HOPS 361-A/IRS 1, although with a substantial contribution from HOPS 361-C/IRS 3. The luminosity of the region suggests that HOPS 361-A, and perhaps HOPS 361-C, are forming intermediate-mass stars.

The powerful bipolar outflow from this region was first identified by Bally (1982) and Wootten et al. (1984). More recently this outflow has been mapped by CO (J=3-2) with ALMA and near-IR H_2 lines (see Figure 4, Walther & Geballe 2019). *Spitzer* 5.2 - 37 micron IRS spectra of the outflow from HOPS 361-C has detected lines of H_2, H_2O, FeII, SiII, SI, SIII, OH, and HD (Melnick et al. 2008). There are at least two protostellar systems driving outflows in the NGC 2071 region: HOPS 361-C/IRS 3, which is a binary (Tobin et al. 2020) and HOPS 361-A/IRS 1. The HST-WFC3 2009 image (Figure 2) will provide the baseline for the proper motion study of the knots. Combining ancillary data from *Spitzer*, *Herschel*, APEX, ALMA, VLA, JCMT-SCUBA, SOFIA-FORCAST, and IGRINS, along with the proposed observations using HST and SOFIA, we will be able to measure the masses, momentum injection rates, and proper motions of the full extent of the outflow and connect it to the protostars and their disks and perhaps to the evolutionary phase.

The 4GREAT observations of four CO transitions (5-4, 8-7, 13-12, and 22-21) and [OI] will be the first far-IR velocity- resolved observations of this region. As the J-shocked gas along the inner boundary of the outflow cavity cools below 5000 K, the cooling of the gas is dominated by [OI] 63.2 micron emission and remains dominated by this line down to fairly low temperatures at any reasonable molecular cloud density (Hollenbach & McKee 1979, 1989). Therefore, the [OI] 63.2 line luminosity is a direct measurement of the outflow mass rate that does not depend on abundance, gas velocity, or extinction. Previous PACS observations, however, often found that the [OI] emission is dominated by extended but spatially varying PDR emission that cannot be accurately subtracted out (Manoj et al. 2013). The 4GREAT observations will allow us to subtract out the narrow lines of emission contributed by the PDR (linewidth ~ few km/s).

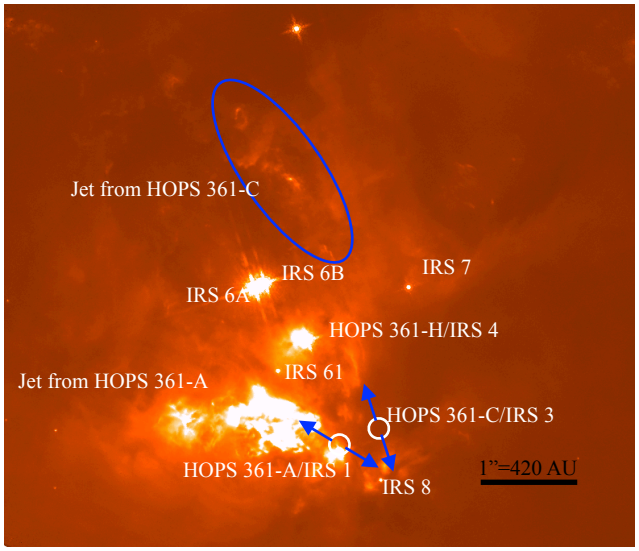

Figure 2: *The 2009 WFC3/IR F160W image of NGC 2071. The HOPS 361 protostars are identified with the blue arrows indicating the outflow directions and IRS components identified in Walther & Geballe (2009).*

In addition, recent GREAT and upGREAT observations of the intermediate-mass outflow OMC2-FIR3 (HOPS 370, Megeath et al. in prep) show relatively narrow line emission for the CO (16-15) and [OI] line. The line profiles suggest that this emission originates in the swept up gas heated by the UV radiation generated by shocks in the outflow. In NGC 2071, the far-IR line profiles of the gas are needed to distinguish between UV heated gas, gas inside the high velocity jets or winds, and the shocked gas where these jets/ winds impact the swept up gas - i.e., the terminal shocks.

The HST data toward the central pointing will be compared with F160W data taken in 2009; these shocks are traced by their emission in the [FeII] 1.66 micron line, which falls within the broadband filter. Our new HST observations will provide measurements of the proper motions of these shocks with high angular resolution needed to measure motions; this is particularly important in regions of clustered star formation like HOPS 361 where we must disentangle multiple outflows. Measurement of the radial velocities of the same shocks as the knots observed by HST in the [OI] and four CO lines will allow us to measure the 3D velocities of their shocks - also elucidating to the structure of the surrounding molecular shocks traced by CO. The observations of the velocities of these shocks will demonstrate the power of combining the angular resolution of the HST with the velocity resolution of SOFIA. The motions of the knots determined from HST proper motions and SOFIA radial velocities will be combined with the shock speeds, derived from the models of the knots' emission spectrum, to provide a detailed picture of the energy, momentum, and mass flows that determine the outflows effect on the cloud, as well as the amount of energy that is radiated away in coolant lines.

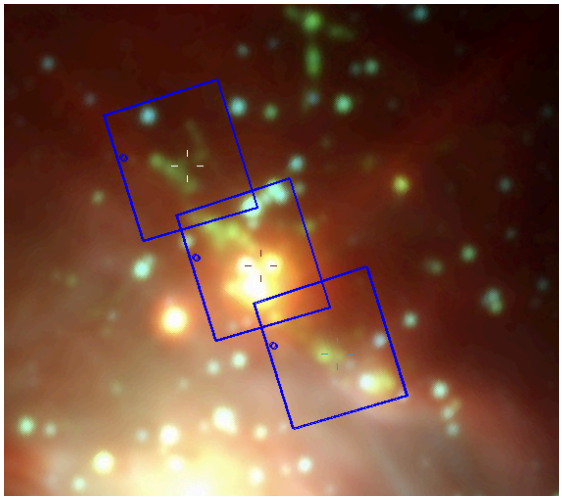

Figure 3: *A Spitzer image with the three HST WFC3/IR pointings (blue boxes) covering the entire extent of the HOPS 361-A and -C outflows.*

Toward all three pointings, the HST data will also provide Paβ as well as dereddened [FeII] emission using the ratio of the [FeII] lines. Application of shock models, such as MAPPINGS 5 (Dopita & Sutherland 2017), to well-resolved, outflow-driven shocks such as these can reveal many key parameters of the outflow, as functions of dynamical time. By themselves, our dereddened [FeII] and H I Paβ images would yield good estimates of the gas-phase Fe/H ratio - a sensitive measure of the vigor of shocks, as Fe is heavily depleted onto dust grains - on very small scales in the shock fronts. Their combination with our [OI] and CO 16-15 line profiles, with or without inclusion of mid-IR lines of [Fe II], [Si II], [S III] and [S I] observed with Spitzer-IRS (Melnick et al. 2008) or observable with EXES, yield good constraints on preshock density, shock speed (rarely the same as flow speed), and the rates at which mass, momentum and kinetic energy cross the shock fronts. These data would lead to comprehensive and accurate constraints on the outflows from the HOPS 361-A/IRS 1 and HOPS 363-C/IRS 3 protostars, as well as strong constraints on the potentially disruptive force exerted on the ambient medium by the outflows. ALMA measurements could accurately trace the swept up gas. In total, this would make this outflow an unparalleled laboratory for understanding protostar outflows, their effect on the ISM, the relevant shock physics, and the origin of the far-IR emission from outflows.

Many unanswered questions still remain on outflows: How do jets and outflow shocks propagate through the surrounding medium and what impact do they have? How does the magnetic field impact the collimation of outflows and relate to the shocks in the region? What is the impact of a group of intermediate- to low-mass protostars on the surrounding dense molecular gas?

Proposed Observations

We will use HST WFC3/IR to observe three pointings towards the HOPS 361 outflows (Figure 3). The emission will be mapped in two lines of J-type shock heated [FeII] and Paschen β. The two lines will give the extinction corrected [FeII] emission, which will measure the mechanical luminosity of the shock. The ~12 year timespan of the WFC3 observations will open the door to look into any morphological changes of the knots themselves. The 4GREAT observations will (Figure 4) map the [OI] (J-type shock) and CO (5-4, 8-7, 31-12, 22-21) line emission, in either 3-point maps or with the HFA in honeycomb mode, as previously detected by Herschel/PACS (Manoj et al. 2013). The higher spectral resolution of 4GREAT will measure the radial velocities of the components, measure the velocity of the lines from the line peak, obtain the line profiles needed to disentangle emission jets, shocks and UV heated entrained gas, and distinguish components from the multiple outflows.

Relating near-IR lines [Fe II] knots, H_2 *Spitzer*, and the far-IR lines, we will further distinguish these components. With this, we will characterize the energetics of the shocks generated by the outflow and better establish the far-IR lines as tracers of the shock mechanical luminosity. Previous data already obtained have constrained the fundamental properties of the protostars, their envelopes, and disks in this region (Furlan et al. 2016; Tobin et al. 2020; Karnath et al. in prep). Understanding all pieces of these protostellar systems is important context to understand the outflow properties associated with those systems.

Observations: i) HST - WFC3/IR will target three pointings to cover the full extent of the outflows (Figure 3). To understand the shocks in the region, we will observe the [FeII] lines (F126N and F164N) and the Paschen β line (128N) tracing the dissociative J-type shocks. These trace the cloud shock, formed as the knot plows into the cloud, and the wind shock, where the outflow encounters the knot. Observing the [FeII] continuum (F167N) and Paschen β continuum (F130N) will pick up scattered light from the protostars and other stars in the region and warm dust. The same integration time (~500 seconds) for each filter with three dithers each will allow the continuum emission to be subtracted out. In order to maximize the potential of the data to carry out shock modeling on the more extended/fainter features in the outflows and proper motion measurements **we ask for 12 orbits in total**. Using 12 orbits instead of 8 may add more than 50% extra value to this dataset from the community's viewpoint. Figure 2 shows the WFC3/IR F160W image from 2009 (priv. comm. Megeath) identifying the jets in the region and the driving protostars.

ii) SOFIA - 4GREAT will spectrally resolve the line profiles and velocity of the far-IR emission by mapping the outflows traced by [OI] 63 microns tracing dissociative J-type shocks and four rotational CO transitions: J = 5-4, J = 8-7, J = 13-12, J= 22-21. For the CO data, the focus will be on the J=13-12 transition; the line is expected to be optically thick in the lower transition and the J=22-21 line is unlikely to be detected. While the [OI] will provide maps of the emission the CO will provide sensitive line profiles at each pointing.

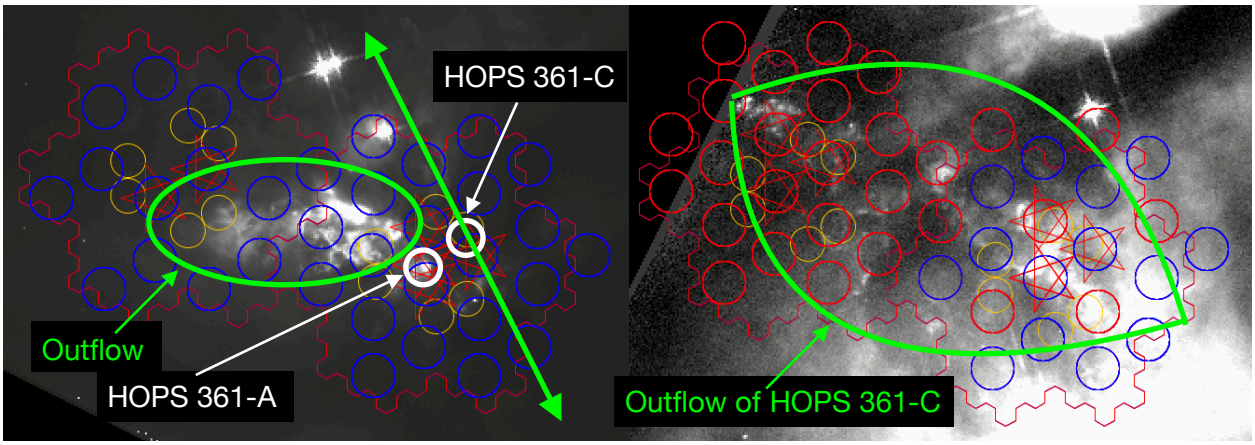

Figure 4: *The 2009 HST WFC3/IR F160W image of the outflows from HOPS 361-A (left) and -C (right) broken into two images to show detail with overlaid 4GREAT footprints. The outflows are encircled in the green to highlight the emission to be detected.* ***Left:*** *The honeycomb beams are outlined in red and the 3-pt method beams are overlaid in blue on the outflow from HOPS 361-A.* ***Right:*** *The honeycomb beams are outlined in red and 3-pt method beams are overlaid in blue and red on top of the NW jet of HOPS 361-C.*

Using Herschel PACS observations, we obtained fluxes in the [OI] and CO 16-15 lines for three regions; the central region, the NE outflow jet, and the SW outflow jet. Due to the low velocity resolution of PACS, the peak antenna temperatures depend on the adopted width of the lines in the PACS data. Assuming 10 km/s widths, similar to [OI] and CO 16-15 lines observed with GREAT toward a similar outflow from HOPS 370, this gives [OI] and CO lines of > 10 K for the central position, 1 and 3.6 K for the NE position, and 0.5 and 0.9 K for the SW position, respectively.

The primary target is the central region (HOPS 361-A) and its outflow (Figure 4, left). To ensure high quality data, we propose to have two observing strategies depending on the brightness of the [OI] line. The observations will start with a single pointing on HOPS 361-A, which is the brightest region with 5 min on+off time to reach ~0.15 K in sensitivity. If the SNR desired is achieved, we will continue observing by tracing the outflows as seen in Figure 4.

If the line is bright (>~3 K) two honeycomb pointings will be observed as seen in Figure 4. For the [OI] line with 1 sigma rms per 1 km/s channel, we estimate that with 1 hour of clock time we will achieve 1800 seconds of on+off integration time and 1800/25 = 72 seconds of on+off time per map point to reach ~0.3 K sensitivity. The map will be gridded after the fact to gain a factor of ~1.5 so the final map sensitivity is ~0.2 K or SNR of 15 at the 3 K threshold.

If the line is faint (~<3 K) two pointings with the 3-point method will be used. This will start with another 5 min on+off time integration of the central position and two offset positions with 10 min of on+off time (20 min clock time). With a total clock time of ~1 hour for all three positions the final sensitivity is ~0.1 K per point. Note that these sensitivities are for the [OI] line, and higher sensitivities will be obtained for the CO 13-12 data, which will essentially give a high S/N line profile at each pointing.

The secondary target is the NE jet from HOPS 361-C (Figure 4, right). Here we plan a similar strategy, although we expect to use the 3-point map as the lines are too weak for the honeycomb maps. The two pointings will extend along the NE jet. Finally, the third position will be the SW jet. Here we will focus on the position showing the peak emission in the Herschel data. We plan to use the three point map given the lower line temperatures at this position.

The total time estimate including overheads, assuming for an upper limit that each position has bright emission and we make a single point observation and the honeycomb are:

- 5 honeycombs, at 3720 seconds per map - 5.2 hours
- 5 single point observations at 720 seconds each - 1.3 hours
- Total 6.5 hours

We have created and designed aors for both strategies (honeycomb and 3-point) so that no time is lost during flight and the maximum amount of science can be achieved in the allotted time given. The tradeoff of using the 3-point method is higher SNR spectra will be achieved but with less spatial information.

Figure 4 shows the proposed footprint of the 4GREAT observations. We note that previous observations of the OMC2-FIR3 (HOPS 370) outflow show that the [OI] and CO 16-15 lines show very similar line profiles, hence we expect that these tracers are tracing the same gas. This science can be **achieved in 6.5 hours of 4GREAT observations**.

Connections to Ancillary Data and Upcoming Observations

ALMA and VLA Observations

As part of the VANDAM survey in Orion (Tobin et al. 2020), HOPS 361-A and other protostars in the region were observed with ALMA (and VLA) including ^{12}CO (2-1) of the inner most parts of the outflows (Figure 5 and 6; Cheng et al. in prep). Radio observations of protostellar outflows place lower limits on mass-loss rates because the radio emission stems from the ionized component of the outflow only. The 4GREAT data will detect the atomic (neutral) component as well as the ionized component leading to a more accurate determination of the mass loss rate in the outflows.

The VANDAM survey (Tobin et al. 2020) also characterized a few hundred protoplanetary disks including HOPS 361-A, -C, -E, -G, and -H. The outflow material is believed to arise from magnetohydrodynamic processes in the rotating star-disk system (see chapter by Bouvier et al. 2007). The launching of jets/outflows is responsible for extracting excess angular momentum from the accretion disk and protostellar winds may affect the disk evolution and planet formation in the disks themselves. The VANDAM observations of the HOPS 361 protostars have measured the disk sizes and masses at the highest resolution possible revealing structures that may have been affected by associated magnetic fields and outflows.

Magnetic Field Observations

The magnetic field of a molecular cloud can impact the collapse of a cloud fragment into a protostar, the formation of the protostellar disk, and the launching of the outflow (see Figure 1). Several observations have been made of the dust polarization within a few 100 AU of HOPS 361-A where the magnetic field is expected to have a significant role in launching the outflow.

Further away from the protostar itself, the magnetic field is expected to be too weak to play a role in the outflow (Hartigan et al. 2007), but this remains unclear.

ALMA Observations: As part of the BOPS survey in Orion (PI: Stephens) carried out ALMA Band 7 polarization observations of 60 Class 0 protostars at 1" resolution. HOPS 361-A and -C were included and the data has just recently been delivered. This small scale magnetic field data are important as the direction of magnetic field at the outflow position it gives some constraint on the magnetic field in relation to shocks. Magnetic fields may play a significant role in regulating the collapse process, disk rotation, and launching outflows.

The power to combine the ALMA (sub)-mm outflow detections with the proposed 4GREAT far-IR outflow observations and the FORCAST photometry (Karnath et al. in prep) presents the opportunity to draw robust conclusions about the time evolution of mass accretion and ejection rates at large and small scales in the HOPS 361 protostars. The spatially and velocity resolved observations from ALMA will help in determining which protostars are driving the outflows responsible for the velocity components in the 4GREAT maps.

HAWC+ Observations: HAWC+ has been previously used to observe NGC 2071 in Band E of 06_0119 (PI: Stephens, Figure 7) and more recent data from 07_0130 (PI: Fanciullo) to detect polarization in Band D and E.

JCMT-SCUBA Observations: Lyo et al. 2021 (submitted) took polarization measurements of NGC 2071 at 450 and 850 microns with SCUBA-2/POL-2 on the JCMT. The paper includes the outflows proposed here but at larger resolution. Archana Soam and Simon Coude are coauthors on this work.

Matthews et al. (2002) obtained SCUBA data on the JCMT detecting polarized thermal emission at 850 microns of the HOPS 361 region. The polarization towards HOPS 361 is quite weak, less than 2% (see Figure 7). The polarization further from HOPS 361 is symmetric and more prominent. Over the entire core region, the vectors exhibit a mean orientation of 20 degrees east of north. Using the Davis-Chandrasekhar-Fermi method, they obtain a magnetic field strength of 59 microGauss.

HST WFC3

Proper motion studies have been carried out on protostellar outflows (e.g., Reiter et al. 2017), but the radial velocity information is missing leaving the full picture incomplete. The HOPS 361 region has previously been observed by WFC3/IR F160W in 2009 (Figure 2) and by comparing the positions of the knots in the outflow over a ~12 year time span will reveal the proper motions. The morphology of the knots themselves will be investigated to determine any changes over ~12 years.

The jet/outflow from HOPS 361-C extends in the northeast-southwest direction of Figures 3 and 4 has been suggested to precess to explain the angular width of the outflow (Carrasco-Gonzalez et al. 2012). However, there is a lack of data to detect any precessional motion or if the outflow is creating the wide-angle seen. The new WFC3 observations will allow

the possible precession to be investigated or if the apparent precessional motion is due to the driving source being a binary system with misaligned outflows/jets.

Possible Opportunities to Advertise and Publish this Data

In order to maximize the impact of the new HST/SOFIA joint proposal program it is important to give the community impactful data that excites and inspires collaborative work. As this team is most familiar with these types of observations and analyses it is important that the team be available to help any interested parties in publishing the data. Additionally, including funding for a student or postdoc to work on the data is essential to making it a top priority and gives a clearly defined timeline for publication.

i) Advertise the newly available data and white papers on both HST and SOFIA websites
ii) Make an announcement(s) at the AAS Winter meeting for both observatories and provide people familiar with the projects to discuss the potential science publishing paths
iii) Post short advertisement in the Star Formation Newsletter once data is taken
iv) Possibly combine funding from both HST and SOFIA to create a postdoc position or part of a position to work on this data and other DDT projects
v) Possibly combine funding from both HST and SOFIA to create an internship for a few months for graduate students similar to the IPAC Visiting Graduate Fellowship program
vi) Inform any tele-talk and colloquium speakers of current and upcoming DDT time for students or postdocs to work on from their collaborations or institutions

Appendix

Upcoming Observations

EXES Observations: EXES observations of the NGC 2071 outflow are planned in an accepted Cycle 8 program (Neufeld 08_0029). These follow-up a previous EXES program performed toward HH7 in which four pure rotational lines of H_2 were detected (Neufeld et al. 2019): the S(4), S(5), S(6) and S(7) lines. Velocity shifts between the ortho- and para-H_2 lines were detected unequivocally by taking advantage of the unique spectral resolution provided by EXES in this waveband. This allows the conversion from para-H_2 to ortho-H_2 to be tracked within the shock wave and provides the most direct evidence to date for the existence of C-type shock waves where the flow velocity varies continuously. The Cycle 8 program targets NGC 2071 at position (05:47:08.21, +00:22:52.7), which is the outflow associated with HOPS 361-C, for a total time of 4.6 hours including overheads, to achieve a minimum S/N of at least 10 per Nyquist-sampled resolution element. If performed, the Cycle 8 observations will place unique constraints on the physics of molecular shocks. The EXES spectra probe the kinematics of the warm, shock-heated H_2 and provide information about the structure of interstellar shock waves and the conversion of para-H_2 to ortho-H_2 within molecular shocks. Future observations with JWST/MIRI will not be able to spectrally resolve the H2 pure rotational lines that EXES can, but will be complimentary in providing exquisite spatial resolution.

References

Arce, H. G., Shepherd, D., Gueth, F. et al. (2007) PPV Proceedings, 245
Bally, J. & Lane, A. P. (1982) ApJ, 261, 558
Bally, J., Reipurth, B., & Davis, C. J. (2007) PPV Proceedings, 215
Bontemps, S., Andre, P., Terebey, S. Et al. (1996) A&A, 311, 858
Bouvier, J., Alencar, S. H. P., Harries, T. J. (2007) PPV Proceedings, 479
Carrasco-Gonzalez, C., Anglada, G., D'Alessio, P. et al. (2012) ApJ, 76, 71
Di Francesco, J., Evans, N. J., Harvey, P. M., et al (1997) ApJ, 482, 433
Dopita, M. A. & Sutherland, R. S. (2017) ApJS, 229, 35
Draine, B. T., Roberge, W. G., & Dalgarno, A. (1983) ApJ, 264, 485
Frank, A., Ray, T. P., Cabrit, S., et al (2014) PPVI Proceedings, 451
Furlan, E., Fischer, W. J., Ali, B. et al (2016) ApJSS, 224, 5
Giannini, T., Nisini, B. & Lorenzetti, D. (2001) ApJ, 555, 40
Gonzalez-Garcia, B. Manoj, P., Watson, D. M. et al. (2016) A&A, 596, 26
Hartigan, P., Frank, A., Varniere, P. et al (2007) ApJ, 661, 910
Hollenbach, D. & McKee, C. F. (1979) ApJS, 41, 555
Hollenbach, D. & McKee, C. F. (1989) ApJ, 342, 306
Karska, A., Herczeg, G. J., van Dishoeck, E. F. et al. (2013) A&A, 552, 141
Karska, A., Kaufman, M. J., Kristensen, L. E. et al. (2018) ApJS, 235, 30
Kaufman, M. J. & Neufeld, D. A. (1996) ApJ, 456, 611
Kounkel, M., Hartmann, L., Laurent, L. et al (2017) ApJ, 834, 142
Kuiper, R., Yorke, H. W., & Turner, N. L. (2015) ApJ, 800, 2
Lada, C. J. (1985) AR&AA, 23, 267
Lee, J.-E., Lee, J., Lee, S. et al. (2014) ApJS, 214, 21
Mannings, V. & Sargent, A. I. (2000) ApJ, 529, 391
Manoj, P., Watson, D. M., Neufeld, D. A. et al. (2013) ApJ, 763, 83
Manoj, P., Green, J. D., Megeath, S. T. et al. (2016) ApJ, 831, 69
Matthews, B. C., Fiege, J. D., & Moriarty-Schieven, G. (2002) ApJ, 569, 304
Matuszak, M., Karska, A., Kristensen, L. E. et al. (2015) A&A, 578, 20
Melnick, G. J., Tolls, V., Neufeld, D. A. et al (2008) ApJ, 683, 876
Nakamura F. & Li, Z.-Y. (2007) ApJ, 662, 395
Neufeld, D. A., DeWitt C., Lesaffre, P., et al (2019) ApJL, 878, 18
Nisini, B., Giannini, T., & Lorenzetti, D. (2002) ApJ, 574, 246
Offner, S. S. R. & Arce, H. G. (2014) ApJ, 784, 61
Reiter, M., Kiminki, M. M., Smith, N. et al. (2017) MNRAS, 470, 4671
Skinner, S. L., Sokal, K. R., Megeath, S. T. et al. (2009) ApJ, 701, 710
Storey, J. W. V, Watson, D. M., Townes, C. H. et al. (1981) ApJ, 247, 136
Tobin, J. J., Sheehan, P. D., Megeath, S. T. et al. (2020) ApJ, 890, 130
van Kempen, T. A., Hogerheijde, M. R., van Dishoeck, E. F. et al. (2016) A&A, 587, 17
Walther, D. M. & Geballe, T. R (2019) ApJ, 875, 153
Watson, D. M., Storey, J. M. V., Townes, C. H. et al. (1980) ApJ, 241, 43
Watson, D. M., Genzel, R., Townes, C. H. et al. (1985) ApJ, 298, 316

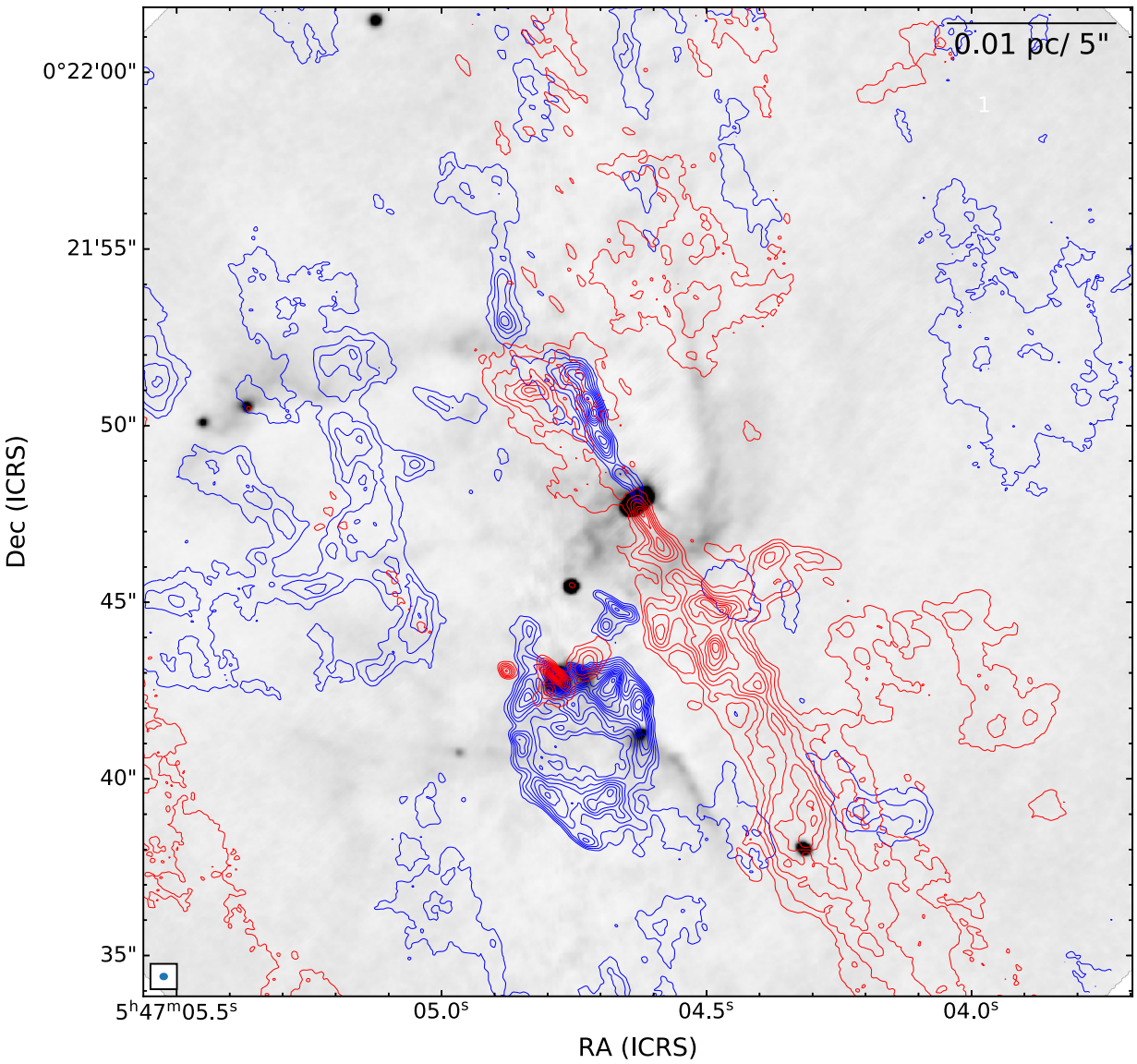

Figure 5: Image from *Yu Cheng. The ALMA outflow data of ^{12}CO (2-1) contours. The velocity ranges are -40 to 0 km/s and +20 to +60 km/s for the blue and red wings, respectively. The gray is the 1.3 mm continuum from ALMA. Data from the Orion VANDAM survey (Tobin et al. 2020).*

Wootten, A., Loren, R. B., Sandqvist, A. Et al. (1984) ApJ, 279, 633

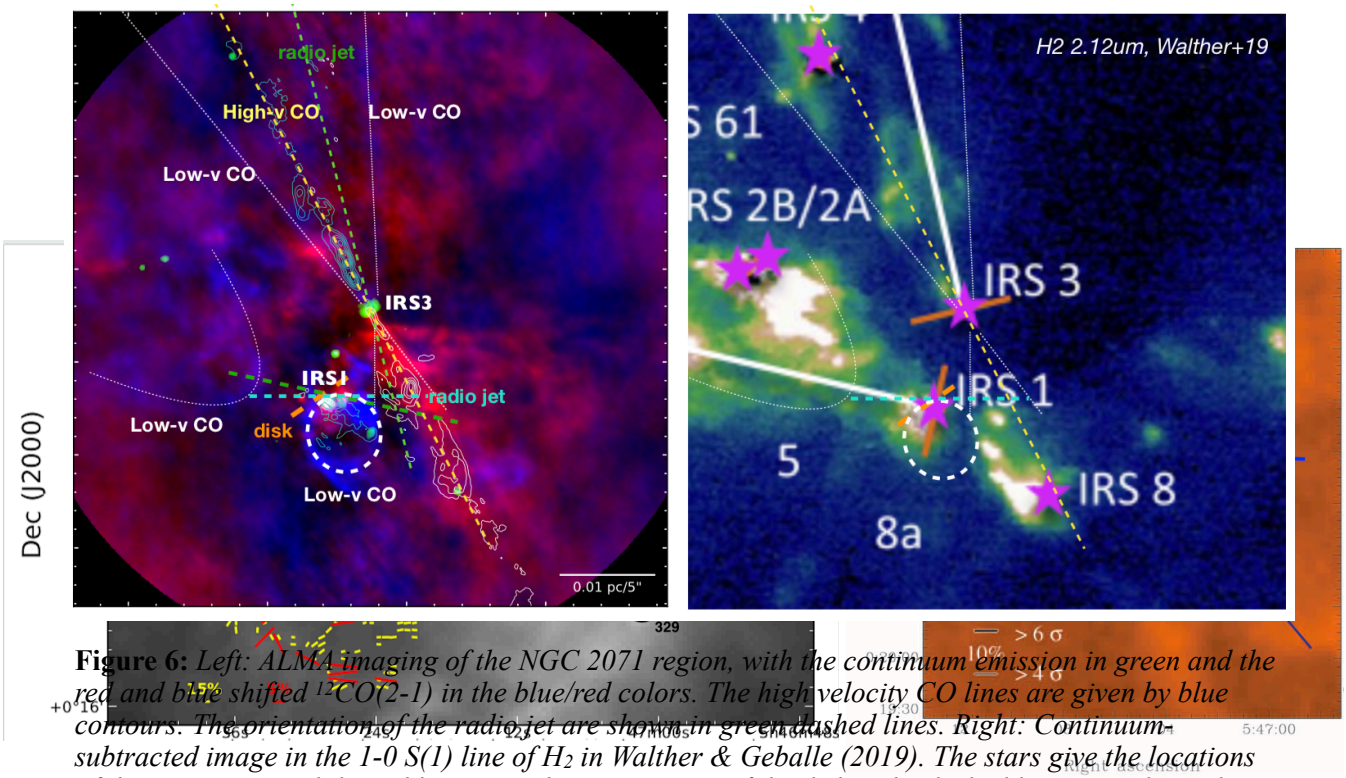

Figure 6: *Left: ALMA imaging of the NGC 2071 region, with the continuum emission in green and the red and blue shifted ^{12}CO(2-1) in the blue/red colors. The high velocity CO lines are given by blue contours. The orientation of the radio jet are shown in green dashed lines. Right: Continuum-subtracted image in the 1-0 S(1) line of H_2 in Walther & Geballe (2019). The stars give the locations of the protostars and the red lines give the orientations of the disks. The dashed lines give the outline of the outflow. Image from Yu Cheng.*

Figure 7: *Left: HAWC+ Cycle 6 Band E observations of NGC 2071 (06_0119, PI: Stephens). The polarization vectors are overlaid in red with the HOPS protostars identified by the black circles. Right: JCMT-SCUBA 850 micron polarization images of NGC 2071 from Matthews et al. (2002). The black vectors show the measured polarization E-vectors and the blue lines show the inferred direction of the*